Learning-induced autonomy of sensorimotor systems

Danielle S Bassett[1,2], Muzhi Yang[1,3], Nicholas F Wymbs[4,5] & Scott T Grafton[4]

Distributed networks of brain areas interact with one another in a time-varying fashion to enable complex cognitive and sensorimotor functions. Here we used new network-analysis algorithms to test the recruitment and integration of large-scale functional neural circuitry during learning. Using functional magnetic resonance imaging data acquired from healthy human participants, we investigated changes in the architecture of functional connectivity patterns that promote learning from initial training through mastery of a simple motor skill. Our results show that learning induces an autonomy of sensorimotor systems and that the release of cognitive control hubs in frontal and cingulate cortices predicts individual differences in the rate of learning on other days of practice. Our general statistical approach is applicable across other cognitive domains and provides a key to understanding time-resolved interactions between distributed neural circuits that enable task performance.

Human skill learning is a complex phenomenon requiring the flexibility to adapt existing brain function to drive desired behavior[1]. Such adaptability requires fine-scale control of distributed neural circuits to transform an activity from slow and challenging to fast and automatic[2]. However, the dynamic manipulation and control of these circuits over the course of learning remains sparsely studied[3].

Previous learning experiments over short time intervals have clearly demonstrated that a few pairwise functional interactions between motor cortical areas, such as between primary motor cortex and supplementary motor cortex, strengthen with skill acquisition[4–6]. However, these local interactions occur within the larger context of the whole brain, which is teeming with thousands or millions of changing functional interactions between hundreds or thousands of large cortical structures. The reconfiguration of this wider dynamic network must be involved in shaping learning over the course of training.

Methods for studying the dynamics of distributed and integrated circuits during cognitive processes remain limited and underpowered[7]. Prior work has relied on studies of specific brain regions or neurons and studies of static network representations of structural or functional circuits or connectomes[8–12], both of which are unable to describe temporal dependence between spatially segregated neural circuits. Initial efforts to utilize both network representations of circuitry and analyses sensitive to dynamics identified gross summary statistics of the whole brain (for example, network flexibility)[13,14], which preclude the specific characterization of individual circuits and their evolution.

Indeed, so far there are no statistically robust methods with which to reliably identify functional modules over short time intervals and characterize their changes over time in individual subjects. Here we introduce a method that has allowed us to address this gap. We used dynamic network neuroscience to probe learning-related changes in inter-regional communication patterns and to link these changes to individual differences in behavioral outcomes. Building on the formalism of network science[15], this approach harnesses a new set of tools from applied mathematics[16] to treat the patterns of communication between brain regions as evolving networks[13,14,17–19] whose reconfiguration dynamics are tightly tied to observable changes in behavior.

We used dynamic network analysis to consider three basic questions about how whole-brain functional networks reconfigure themselves during skill learning[13,14,17,20,21]. First, are there sets of brain regions (or 'modules') that preferentially interact with one another during task performance, and if so, do these modules or their interactions change with learning? Basic intuition suggests that motor output areas might form a task-relevant module. Because sensory-guided behavior becomes less of a critical driver for some motor skills in late learning[22], one might also hypothesize that sensory regions form a task-relevant module, whose integration with the motor modules changes with training. Second, what role does association cortex have in task performance? During early learning, performance can be enhanced by explicit strategies, cognitive control and guided attention, but with extensive practice, these enhancements are no longer needed[23,24] and cognitive control circuits become less engaged[25]. One might therefore expect that the interaction between associative and motor modules changes with training. Third, could the interplay between task-relevant (for example, motor and sensory) modules or the involvement of association cortex explain the dramatic differences between individual people in the capacity to learn? Given that initial skill acquisition has heightened attentional demands[23,24] and that individual differences in cognitive control mechanisms predict learning in other domains[26], one might hypothesize that slow learners rely on associative systems more or for longer periods of time than do fast learners.

We addressed these questions by quantifying changes in putative functional modules induced by motor learning. We built temporal

[1]Department of Bioengineering, University of Pennsylvania, Philadelphia, Pennsylvania, USA. [2]Department of Electrical and Systems Engineering, University of Pennsylvania, Philadelphia, Pennsylvania, USA. [3]Applied Mathematics and Computational Science Graduate Group, University of Pennsylvania, Philadelphia, Pennsylvania, USA. [4]Department of Psychological and Brain Sciences and UCSB Brain Imaging Center, University of California, Santa Barbara, Santa Barbara, California, USA. [5]Human Brain Physiology and Stimulation Laboratory, Department of Physical Medicine and Rehabilitation, Johns Hopkins Medical Institution, Baltimore, Maryland, USA. Correspondence should be addressed to D.S.B. (dsb@seas.upenn.edu).

Received 3 November 2014; accepted 11 March 2015; published online 6 April 2015; doi:10.1038/nn.3993

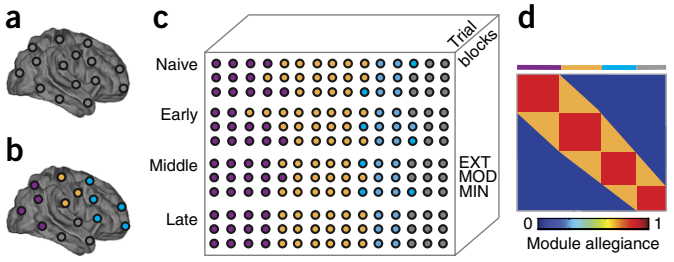

Figure 1 Schematic of methods. (**a**) We parcellated the brain into 112 cortical and subcortical regions based on the Harvard-Oxford atlas. (**b**) We calculated the functional connectivity between these regions to create a functional network and clustered regions within the functional network using community-detection techniques. (**c**) We collated the community assignments ('partitions') across different time scales of learning (naive, early, middle and late), different depths of training (extensive (EXT), moderate (MOD) and minimal (MIN)) and different subjects. (**d**) We created a module-allegiance matrix indicating the probability that any two regions will be classified into the same network community.

networks from functional magnetic resonance imaging (fMRI) data acquired from subjects learning motor sequences (discrete sequence production; **Supplementary Fig. 1**) by (i) subdividing the brain into 112 cortical and subcortical areas (nodes) and (ii) calculating the functional connectivity (edges) between pairs of regions in independent time windows (2–3 min in duration corresponding to trial blocks) during task performance (**Fig. 1a**). Using a clustering approach designed for time-evolving networks[27], we extracted groups of brain regions (network communities) that were coherently active in each time window, with each group putatively responsible for a specific cognitive function[28] (**Fig. 1b**). Using this approach, we obtained subject-specific communities at multiple trial blocks over the course of 6 weeks (four scan sessions; **Supplementary Fig. 2**) of sequence learning, during which subjects practiced a set of sequences at three levels of training intensity (extensive, moderate and minimal), for a total of 12 training levels (**Fig. 1c**). This experimental construct enabled us to distinguish between time scales of learning (over the 12 training levels) and time periods of learning (in the four sessions over the 6 weeks of training). Extracting subject-specific communities across these time scales allowed us to ask how large-scale interconnected systems adapt during motor skill acquisition, a question that cannot be addressed by traditional, activation-focused approaches. It also enabled us to identify characteristics of that adaptation that predict individual differences in learning.

RESULTS

Summary architecture of learning

We first sought to address the question, "Are there sets of brain regions (or modules) that preferentially interact with one another during task performance?" To answer this question, we examined the brain network architecture that was consistently expressed across motor skill learning. For each pair of brain regions, we computed a normalized value of module allegiance representing the probability that area i and area j were assigned to the same functional community by time-resolved clustering methods[13,27] (see Online Methods). More specifically, we constructed a matrix $\boldsymbol{T}$ whose elements T_{ij} indicated the number of times that nodes i and j had been assigned to the same community in the set of functional brain networks constructed from all subjects, scanning sessions, sequence types and trial blocks. We then computed $\boldsymbol{P} = (1/C)\boldsymbol{T}$, where C is the total number of partitions, to obtain the module-allegiance matrix $\boldsymbol{P}$, whose elements P_{ij} give the probability that area i and j are in the same community (**Fig. 1d**). The **Supplementary Note** presents a description of the utility of the probability matrix P_{ij} in comparison to that of the functional connectivity matrix F_{ij}.

The module-allegiance matrix is a summary of the brain network architecture accompanying learning. In our study, this architecture displayed several interesting anatomical features (**Fig. 2a**), including two sets of brain regions that were consistently grouped into the same network community. We refer to these two sets as putative functional modules. One of these modules is composed of primary and secondary sensorimotor regions (**Fig. 2b**), and the other module is composed of primary visual cortex (**Fig. 2c**). **Table 1** shows region labels associated with the two modules. The dissociation of these two modules indicates that brain areas in these two systems display significantly different time courses of blood oxygenation level–dependent (BOLD) activation.

We refer to the remaining regions of the brain—which did not participate in the motor and visual modules—as constituting a non-motor, non-visual set. These areas did not tend to show consistent allegiances to any putative functional modules, which indicates that their BOLD time courses are significantly different from those characterizing the motor and visual modules, and significantly different from one another. We observed that the regions in this set tended to have split allegiances: a pair of regions tended to have a 29% probability of belonging to the same community, which is much lower than that observed for the visual (80%) and motor (65%) modules. We can interpret this difference by noting that the visual and motor modules contain areas required for task execution, whereas the non-motor, non-visual set includes areas required for higher order cognitive processes such as attention, executive function and cognitive control. This suggests that cortices relevant for cognitive processes might be functionally coherent only transiently, whereas cortices relevant for task execution are functionally coherent consistently throughout learning.

Dynamic architecture of learning

We next asked, "Do these modules or their interactions change with learning?" To answer this question, we constructed separate

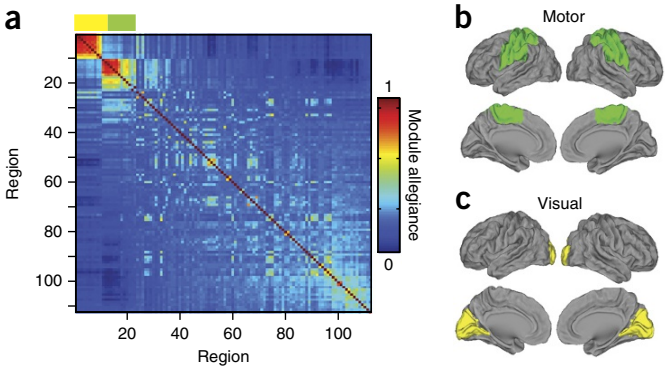

Figure 2 Summary architecture of learning. (**a**) The module-allegiance matrix indicating the probability that two nodes will be located in the same functional community across subjects, scanning sessions, sequence types and trial blocks. (**b**,**c**) The module-allegiance matrix displays two putative functional modules composed of brain regions that are consistently grouped into the same network community: one composed of primary and secondary sensorimotor areas (**b**), and one composed of primary visual cortex (**c**). Brain regions in **a** were ordered to maximize strong associations along the diagonal. For brain-surface visualizations we used Caret software (http://brainvis.wustl.edu/wiki/index.php/Caret:About).

Table 1 Brain areas in motor and visual modules

Motor	Visual
L,R precentral gyrus	L,R intracalcarine cortex
L,R postcentral gyrus	L,R cuneus cortex
L,R superior parietal lobule	L,R lingual gyrus
L,R supramarginal gyrus, anterior	L,R supracalcarine cortex
L,R supplementary motor area	L,R occipital pole

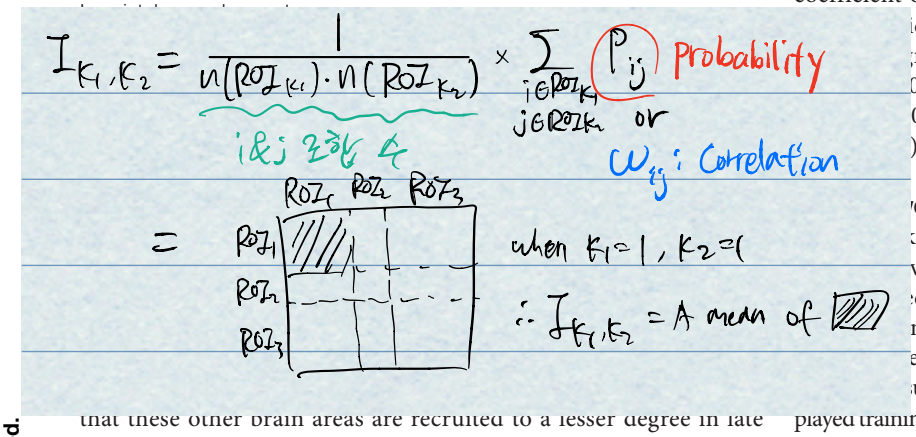

that these other brain areas are recruited to a lesser degree in late learning than in early learning.

To quantify these observations, we estimated the recruitment and integration of the three groups of brain areas defined from the module-allegiance matrix summarizing task-based network architecture (see the preceding subsection): the motor module, the visual module and the non-motor, non-visual set. Let $C = C_1,\ldots,C_k$ be the partition of brain regions into these three groups. Then $I_{k_1,k_2} = (\Sigma_{i\in C_{k_1}, j\in C_{k_2}} P_{ij})/(|C_{k_1}||C_{k_2}|)$ is the interaction strength between group C_{k_1} and group C_{k_2}, where $|C_k|$ is the number of nodes in group C_k. To compute the average recruitment of a single group to the task, we let $k_1 = k_2$. To compute the average integration between two different groups ($k_1 \neq k_2$), we calculated the normalized interaction strength $I'_{k_1,k_2} = I_{k_1,k_2}/\sqrt{I_{k_1,k_1}I_{k_2,k_2}}$, which accounted for statistical differences in group strength. We refer to both recruitment and integration more generally as 'brain network diagnostics'. For additional mathematical details, see the **Supplementary Note**.

Recruitment and integration in the motor and visual modules and in the non-motor, non-visual set were differentially modulated by training. Motor and visual modules were recruited steadily throughout task practice (**Table 2**). However, the integration between motor and visual modules decreased with the number of trials (**Fig. 4a**). This decaying motor-visual integration was not significantly correlated with motor or visual recruitment (Spearman's rank correlation; $P \geq 0.05$) and suggested that motor and visual systems become more autonomous with training. As motor and visual autonomy increased, the recruitment of areas in the non-motor, non-visual set decreased (**Fig. 4b**), suggesting that task performance in later learning does not require that higher order association areas coordinate their functions. (See **Supplementary Figs. 3** and **4** for the robustness of these observations to different methodological choices.)

To quantify these observations, we defined the training-dependent modulation of brain network diagnostics as $-r$, where r is the Pearson coefficient of correlation between the logarithm of the number of ...iced and the diagnostic value. Motor-visual integration ...nificant training-dependent modulation ($r = -0.93$, ...0^{-6}), as did non-motor, non-visual recruitment ($r = -0.96$, ...0^{-7}). These changes were evident not only from the base-...) condition but also steadily throughout learning.

...el correlates of performance and learning

...ked, "Could the interplay between task-relevant modules ...vement of association cortex explain the dramatic differ-...en individual people in the capacity to learn?" To answer ...n, we performed a more fine-grained analysis at the indi-...ect level.

...ual integration and non-motor, non-visual recruitment displayed training-dependent modulation at the single-subject level. However, the strength of this modulation varied across individuals, indicating that some individuals showed stronger growth in sensorimotor autonomy than others. We hypothesized that individuals whose brain networks displayed greater sensorimotor autonomy during training would learn better than those whose brain networks maintained strong motor-visual integration and non-motor, non-visual recruitment in late learning.

To test this hypothesis, we examined the relationship between a statistic summarizing learning in individual subjects and the strength of training-dependent modulation. To calculate the learning parameter, we defined the movement time as the period from the first to the last button press for a given sequence. We then defined the statistic of the learning rate as the exponential drop-off parameter of the movement times[13], collated from home training sessions over the course of the 6-week experiment. We did not observe a significant relationship between training-dependent modulation of motor-visual integration and learning rate ($r = 0.42$, $P = 0.0650$). This suggested that the separation between motor and visual modules was driven by task practice (which was common across the group) rather than learning rate (which differed across participants). Conversely, we observed a strong correlation between training-dependent modulation of non-motor, non-visual recruitment and learning rate ($r = 0.59$, $P = 0.0062$; **Fig. 5**). This suggested that individuals who were able to discontinue coordinated activity across extraneous brain areas in the non-motor,

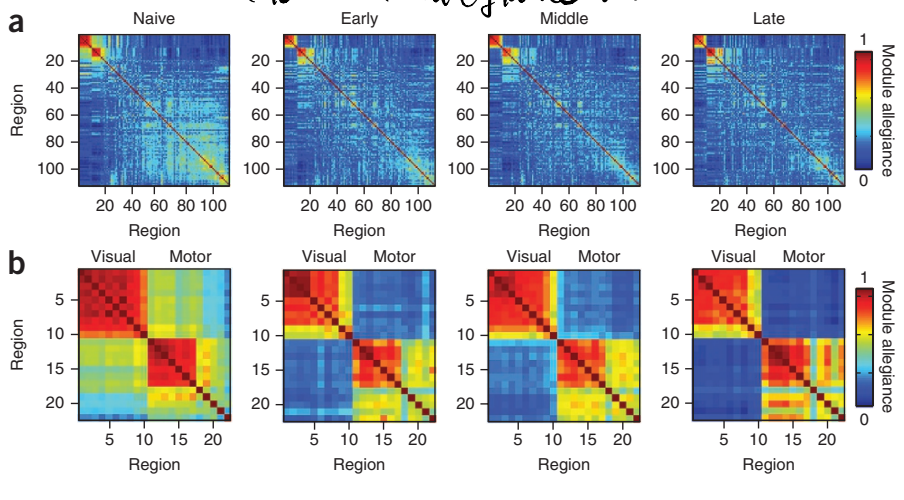

Figure 3 Dynamic brain architecture associated with task practice. (**a**) In naive, early, middle and late learning, the motor and visual modules evident in the stable architecture (**Fig. 2a**) were also present. We observed a decrease in the strength of allegiance between regions in the non-motor, non-visual set. (**b**) Magnified views of the motor and visual modules from **a** demonstrating the decrease in the strength of allegiance between these modules as learning progressed.

Table 2 Scans, sequence type and training level

	Naive	Early	Middle	Late
MIN sequences	50	110	170	230
MOD sequences	50	200	350	500
EXT sequences	50	740	1,430	2,120

Shown is the number of trials (i.e., 'training level') of each sequence type completed after each scanning session averaged over the 20 participants. MIN, minimally trained; MOD, moderately trained; EXT, extensively trained.

non-visual set over the course of training were better able to learn than individuals who maintained coordinated activity across these extraneous areas through later learning. (See **Supplementary Fig. 5** for robustness to methodological choices.)

Effect of baseline state

In the two preceding sections, we report the degree of release of (i) the motor and visual modules from one another and (ii) the non-motor, non-visual set. An important potential driver of this release is the amount of motor-visual integration or of non-motor, non-visual recruitment in the baseline condition—day 1, the naive state. Will individuals who display greater motor-visual integration at baseline also show greater training-dependent release (as measured by the Pearson correlation between the motor-visual integration and the log of the number of trials practiced)? Similarly, will individuals who display greater non-motor, non-visual recruitment at baseline also show greater training-dependent release (as measured by the Pearson correlation between the non-motor, non-visual recruitment and the log of the number of trials practiced)? To address these questions, we directly assessed the relationship between the magnitude of recruitment or integration at baseline and the degree of release. We observed that individuals who displayed greater motor-visual integration during early learning (day 1) also showed greater release as estimated by the training-dependent modulation value (Pearson correlation coefficient $r = -0.72$, $P = 0.00036$). Similarly, individuals who displayed greater non-motor, non-visual recruitment during early learning (day 1) also showed greater release as estimated by the training-dependent modulation value ($r = -0.57$, $P = 0.0087$). Despite the relationship between recruitment or integration in the baseline condition (day 1) and the degree of release, baseline recruitment of the non-motor, non-visual set was not a predictor of individual differences in learning rate ($r = 0.30$, $P = 0.19$).

A network driver of individual differences in learning

Our observation that the training-dependent modulation of non-motor, non-visual areas was correlated with individual differences in learning was based on system-scale measurements. We next asked

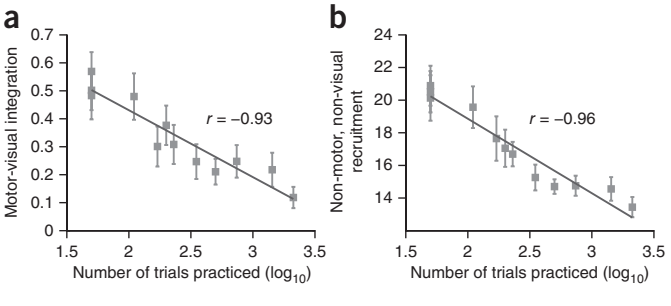

Figure 4 Recruitment and integration were modulated by training. (**a**,**b**) Motor-visual integration (**a**) and non-motor, non-visual recruitment (**b**) as a function of the number of trials practiced. Solid diagonal lines indicate the best linear fit, and *r* values indicate Pearson correlation coefficients. Error bars indicate s.d. of the mean across participants.

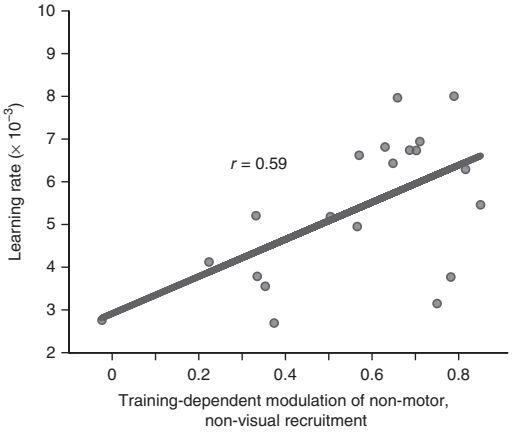

Figure 5 Individual differences in brain network architecture map to task learning. Scatter plot of learning rate and training-dependent modulation of non-motor, non-visual recruitment ($r = 0.59$, $P = 0.0062$).

which specific elements—or functional connections—within that system were driving the observed differences.

To address this question, we calculated the training-induced modulation of each edge connecting pairs of brain areas in the non-motor, non-visual set for each participant and asked whether this value was correlated with the learning-rate parameter estimated from the at-home practice sessions. We collated the set of edges for which this correlation between brain (during scan) and behavior (during separate at-home practice sessions) was significant ($P < 0.05$, uncorrected; Pearson's *r*) and referred to this set of edges collectively as the 'driver' network.

The driver network, which spanned approximately 96% of the non-motor, non-visual set, was composed of 180 functional connections whose changes in connectivity were found to correlate with individual differences in learning (**Fig. 6a**). These connections were distributed asymmetrically throughout the network: a few brain areas boasted many connections in the driver network, but most brain areas had only a few. This observation could be quantified by the regional strength, defined as the sum of the weights of the edges emanating from that area; recall that the weights of the driver network were represented by the Pearson correlation coefficient *r* between the training-induced modulation of that edge and the learning rate. Consistent with our qualitative observations, the distribution of strength values over brain areas was highly skewed ($s = 1.89$)—significantly more so than would be expected in a random-network null model (non-parametric test $P = 0.00009$; see the **Supplementary Note** for statistical details). We observed that areas of high strength in the driver network were predominantly located in the frontal cortex, anterior cingulate and basal ganglia including the nucleus accumbens and putamen (**Fig. 6b**), suggesting that the training-induced release of a frontal-cingulate system predicts individual differences in learning.

DISCUSSION

Here we address the hypothesis that long-term skill acquisition requires changes in the recruitment and integration of functional systems[29]. We acquired fMRI data during the performance of a motor sequence task that was practiced over 6 weeks. We used new network-analysis algorithms to map data-derived functional modules of synchronized brain areas to anatomical boundaries, quantify the recruitment of each module separately and calculate the functional integration between modules as a function of training intensity. We observed that motor areas and primary visual

areas formed two separate, functionally cohesive modules whose recruitment did not change with training but whose integration decreased as sequence performance became more automatic. We also observed that the remaining brain areas (which we refer to as the non-motor, non-visual set) displayed decreasing integration as training progressed, and individual differences in the extent of this decrease—particularly in the fronto-cingulate system—predicted individual differences in learning during separate at-home training sessions.

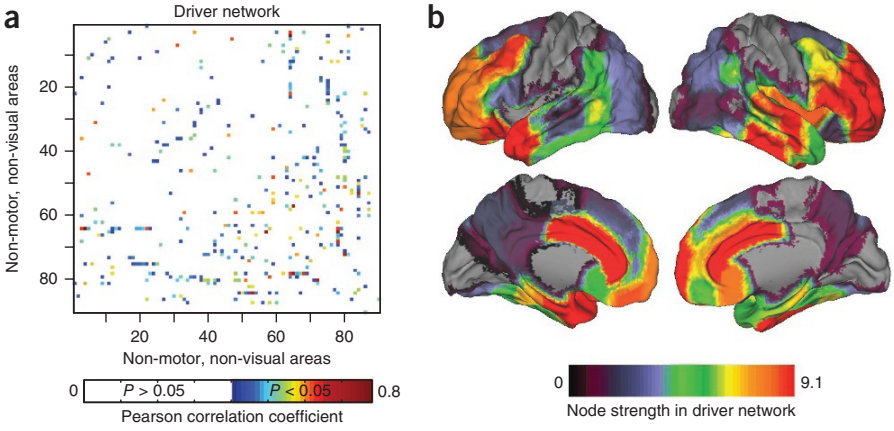

Figure 6 The release of a fronto-cingulate control network predicts individual differences in learning. (**a**) Elements in the driver network are given by the statistically significant ($P < 0.05$, uncorrected) Pearson correlation between individual differences in training-induced modulation and individual differences in learning. Colors indicate the magnitude of the Pearson correlation coefficient. (**b**) The strength of brain areas mapped onto the cortical surface using Caret. The strength of area *i* is given by the sum of column *i* in the driver network. Warm colors indicate high strength in the driver network, and cool colors indicate low strength in the driver network. For brain-surface visualizations we used Caret software (http://brainvis.wustl.edu/wiki/index.php/Caret:About).

Task-based network architecture

The summary network architecture of learning shows significant differences from the architecture observed in resting-state functional connectivity[28,30]. In the resting state, subjects tend to display dense functional connectivity within but not between well-known circuits, including the default mode, fronto-parietal, visual and attention systems. Our work demonstrates that the structure of task-based functional connectivity can be quite different, displaying recruitment of only a couple of systems (for example, motor and visual) that are highly integrated.

Learning-induced changes in sensorimotor systems

How sensorimotor areas change their activity during motor skill learning has been the topic of extensive study in recent years[29]. Collectively, these studies show that in early (fast) learning, sequential motor tasks (i) decrease the magnitude of the task-evoked BOLD response in the dorsolateral prefrontal cortex, primary motor cortex and presupplementary motor area[31,32] and (ii) increase the magnitude of the task-evoked BOLD response in the premotor cortex, supplementary motor area, parietal regions, striatum and cerebellum[31,33,34]. Long-term sequence learning is linked to (i) increases in the magnitude of the task-evoked BOLD response in primary motor cortex[31], primary somatosensory cortex[31], supplementary motor area[35] and putamen[31,35] and (ii) decreases in the magnitude of the task-evoked BOLD response in lobule VI of the cerebellum[35].

In contrast to these studies, we uncovered network adaptations across a continuum of learning, rather than examining early or late learning alone. Moreover, we probed the dynamic, learning-induced integration and release of distributed cognitive systems, processes that are inaccessible in studies of task-related activity alone. Activity and functional connectivity provide two different views of changes in brain function, as evidenced by recent work in learning[13], memory[36], disease diagnosis[30], intervention[37] and genetics[38]. As a complement to task-related activity, functional connectivity has the added advantage of providing information on the inter-regional interactions[4] that form the structure of cognitive models of learning[29].

Our results suggest that motor and visual systems transition from being heavily integrated early in learning to functioning as autonomous units later in the process, such that each system performs independent computations hallmarked by characteristic temporal profiles of BOLD activity. (See **Supplementary Fig. 6** for quantitative relationships between module dissociation and BOLD activation, and see **Supplementary Fig. 7** for quantification of the change in sensorimotor autonomy induced by learning.) This increasing autonomy is consistent with the functional requirements of skill acquisition. In our study, during early learning subjects were required to master multiple tasks that necessitated the integration of vision and motion: the use of a response box, decoding of the visual stimulus, performance of precise movements, balancing of attention between visual stimuli and switching between different sequences of movements. In addition, until they developed an internal model or representation of each ten-element sequence, they were dependent on each visual cue to guide subsequent key presses. Once a sequence was well learned, the only visual information needed was the initial cue indicating which sequence to perform. At this point, subjects were able to execute an entire sequence in an extremely rapid, predictive manner, without reliance on visual instruction from individual key-press stimuli. Furthermore, the enhancement of sensorimotor autonomy is consistent with a neural-efficiency hypothesis. Such a hypothesis could suggest that as learning progresses, the cognitive resources utilized early in learning are no longer needed. Instead, the cortical system will tend to economize resources[24,25] and limit unnecessary communication and transmission to enable automaticity.

In contrast to evidence demonstrating that regional activity within the motor cortex decreases as a function of training[29], we observed that the recruitment of the motor and visual systems did not change significantly as a function of the number of trials. The differences between the two sets of results probably arise from the nonequivalence of activity and connectivity[36]: highly active nodes need not show high functional connectivity to the rest of the brain, and less active nodes need not show less functional connectivity to the rest of the brain. On the basis of our results and previous work, we conclude that although the activity of some motor regions may decrease with practice, the functional connectivity between motor regions remains strong throughout training. For a quantitative assessment of practice effects in motor and visual regions as opposed to modules, see **Supplementary Figure 8**.

A fronto-cingulate network predicts individual differences in learning

As the autonomy of motor and visual systems increases, recruitment of the remaining areas of the brain decreases. Individual differences

in the recruitment of the non-motor, non-visual network (measured during fMRI scans) were correlated with individual differences in learning (measured during at-home training sessions): individuals who were able to disband this network during task practice learned better than those who were not. Such a correlation was not observed between learning and motor-visual recruitment or integration. These results are consistent with those of a prior study linking the BOLD amplitude of motor and premotor cortices with task performance but not with learning[39]. Thus, whereas motor-visual systems are required for general processes such as task execution, the non-motor, non-visual network encapsulates subject-specific processes, including individual differences in learning.

We further identified the distributed network of individual functional connections whose training-dependent release (as measured during fMRI scans) predicted individual differences in learning (measured during at-home training sessions). These connections emanated predominantly from frontal and anterior cingulate cortices, two hubs of known cognitive control systems, the fronto-parietal and cingulo-opercular systems. These two systems are characterized by different functional connectivity patterns at rest[28] and are thought to support distinct functional roles[40]: task-switching[41] and task-set maintenance[42], respectively. This top-down control varies depending on the organism's goals and the characteristics of the given task[43]. Prior work suggests that although too much cognitive control can impede learning[44], at appropriate levels of engagement, the two processes interact symbiotically by modulating common anatomical structures (prefrontal cortex and basal ganglia)[45]. It is intuitively plausible that cognitive control is particularly critical during early skill acquisition[23,24] and becomes less so as skills reach automaticity. This idea is supported by our results, which show that these two hubs of known cognitive control systems became disengaged from the rest of the network over the 6 weeks of training.

Importantly, the neurophysiological processes that we have described were extracted from four scanning sessions held every 1.5–2 weeks over a 6-week period of task practice. The behavioral estimates of learning, in contrast, were extracted from home training sessions that took place on the days between scans. The temporal separation of the data from the scanning sessions (which we used to estimate recruitment and integration) and from the home training (which we used to estimate learning) ensures that these results are predictive rather than simply correlative. Prior reports of neurophysiological predictors of learning have focused on either gross network characteristics[13,14] or isolated functional connections[6], thereby inhibiting interpretations at the level of dynamically integrated cognitive systems. Here we employed a new set of methodological approaches that enabled us to identify the cognitive networks engaged during the task, track changes in the recruitment and integration of networks during task practice, extract a network of functional interactions driving individual differences in learning, and confirm the statistical significance of this driver network using nonparametric null models. Collectively, these approaches enabled us to link characteristics of network adaptivity to known cognitive systems and the broader cognitive neuroscience literature describing their functions.

Methodological considerations

Typical fMRI-analysis approaches identify task-related changes in the activation of various brain regions. Here we used a distinct but complementary network-based approach. We have identified changes in functional connectivity between brain regions and shown how those changes in connectivity related to differences in individual learning rates. It is important to note that questions regarding the organization of functional connectivity patterns cannot be addressed with standard fMRI-analysis approaches based on the general linear model, which measure only the magnitude of task-locked activity. Instead, such questions require the use of connectivity-based approaches, such as those that utilize tools, statistics and diagnostic approaches from network science. **Supplementary Figure 9** shows quantitative assessments of the distinct insights provided by analyses of activation levels and functional connectivity.

In choosing and developing the approaches used in this work, we considered several factors. First, we chose to perform a whole-brain analysis, rather than examine a handful of regions displaying task-related BOLD activation, to enhance our ability to detect features of inter-regional communication patterns that either directly or indirectly support task performance and motor learning. Second, we chose to examine functional connectivity rather than BOLD activity, to enable us to probe the recruitment and integration of cognitive systems engaged in motor skill acquisition over both early and late learning periods. Third, we chose to focus on network modularity and the changes in putative functional modules during skill learning, rather than on more global or local graph metrics, which are less easily interpreted in the framework of known cognitive systems. Finally, we chose to present and characterize module-allegiance matrices rather than individual partitions, because they more accurately display the inherent overlaps between putative functional modules, which, rather than forming independent systems, can display behaviorally relevant interactions that can differ across individuals and change over the learning period.

Several methodological choices deserve additional consideration. First, region size has been shown to have a considerable effect on structural network architecture as estimated with other imaging modalities. In the **Supplementary Note**, we show that our results cannot be attributed to differences in region size between the modules. Second, different parcellation schemes—particularly those with smaller regions—may provide additional clarity. **Supplementary Figures 10–13** show that our results were robustly present in a finer-grained parcellation scheme composed of 626 cortical, subcortical and cerebellar regions.

Third, the experimental block design affects the coherence between brain regions: two brain regions might be active during the trial but quiet during the intertrial interval, leading to a characteristic on-off activity pattern that is highly correlated with all other regions that also turn on with the task and off during the intertrial interval. The frequency of this task-related activity was included in our frequency band of interest (0.06–0.12 Hz), and therefore it probably affected the observed correlation patterns between brain regions in a single time window. Note, however, that our investigations of dynamic network architecture probed functional connectivity dynamics at much larger time scales (40–60 repetition times), and the associated frequencies were an order of magnitude smaller (0.0083–0.012 Hz). At these longer time scales, one can probe the effects of both early learning and extended learning independently of block-design effects, but it will not be possible to assess transient network recruitment at the scale of intertrial changes.

Fourth, two common approaches to network analysis are (i) the examination of a fully weighted network and (ii) the examination of a weighted network that has been thresholded using some test for the statistical significance of individual edges in the network[18]. **Supplementary Figures 3–5** show that our results were robust in both thresholded and unthresholded module-allegiance matrices. When introducing any new method, it is important to ask whether similar results could have been uncovered using a simpler approach. **Supplementary Figure 14** and the **Supplementary Note** show

that our module-allegiance matrices provided a level of sensitivity to learning-related changes in brain network architecture that is not observed in functional connectivity matrices alone. Because the module-allegiance matrix represents information about the network topology only, it is unaffected by measurement noise that may change the mean or distribution of functional connectivity values.

This study stands in contrast to prior studies of functional-network organization during human motor skill learning in terms of both methodological innovation and neurophysiological insights. Unlike the global statistics such as flexibility used in other studies[13,14], we defined a meso-scale object (the module-allegiance matrix) and associated statistics (recruitment and integration) that quantified a brain region's membership in coherent network communities. We used this novel approach to extract individual communities and their dynamics in a statistically robust fashion, facilitating a direct examination of how network reconfiguration relates to underlying brain systems. Furthermore, in contrast to studies of early learning[13,20], here we utilized a far longer training period (6 weeks as opposed to 3 d), which led to much deeper skill learning. Thus, the results of this study should be more readily generalizable to a broad range of motor behaviors that require extensive practice for competence to occur.

Although our results are predictive in the sense that the release of the fronto-cingulate network measured during fMRI sessions predicted individual differences in learning rate measured during at-home training sessions, the question of temporal prediction remains an open one. Does cognitive-control release induce learning, or does learning lead to cognitive-control release? Although our data do not speak directly to this question, prior work suggests the former. The evidence that cognitive control can impede learning[44] suggests that a release of cognitive control would enhance learning. Such a proposal is directly supported by the results of a recent transcranial magnetic stimulation study, which show that silencing the activity of dorsal-lateral prefrontal cortex (via inhibitory theta-burst transcranial magnetic stimulation) facilitates motor sequence learning in healthy human participants[46]. On the basis of the existing literature, we propose that early cognitive-control release enables later learning. However, more research is required to clarify the relative importance of early release versus early network engagement of motor-visual and cognitive-control systems.

Broader implications for cognitive and clinical neuroscience

Our results highlight several important opportunities for studying the cognitive neuroscience of learning. The traditional mapping of single functions to single brain areas is probably an overly simplistic account of cognitive function, unable to accurately depict its true complexity[7]. Network science provides a complement to traditional univariate contrast analyses by providing access to neurophysiological processes that would otherwise be hidden. These processes include changes in BOLD activity and connectivity that occur over the time course of skill acquisition (see **Supplementary Fig. 9** for quantitative relationships between activity and connectivity in these data). Indeed, our results suggest that single brain areas are unlikely to map to single cognitive functions in all task conditions and at all times. Instead, brain regions may alter their allegiance to putative functional modules across time and in different task states according to the most relevant association for the cognitive process at hand[14]. We speculate that the further development of empirical, computational and theoretical methods for probing these intricacies is likely to be of increasing relevance in addressing the challenging questions that currently face cognitive neuroscience.

Our findings in a healthy adult cohort could also inform the understanding of and hypotheses regarding disease- and injury-induced changes in the abnormal brain. Neurodegeneration, movement disorders and stroke can be associated with large-scale reorganization of the motor system[47]. In these scenarios, both individual circuits and their interactions with one another can be altered[48]. Our results suggest that the anatomical (in motor, visual or cognitive control systems) and topological (within versus between cognitive and sensorimotor systems) locations of these alterations account for a substantial amount of variance in individuals' behavioral responses to rehabilitation and treatment[49] (see **Supplementary Fig. 15** for an assessment of individual differences in other behavioral variables), which could inform therapeutic manipulations of circuits in the form of noninvasive brain stimulation[50].

CONCLUSIONS

The dynamic integration of distributed neural circuits necessary to transform the performance of a motor skill from slow and challenging to fast and automatic has evaded description because of statistical and mathematical limitations in current analysis frameworks. Here we used dynamic network neuroscience approaches to expose the learning-induced autonomy of sensorimotor systems and uncover a distributed network of frontal and anterior cingulate cortices whose disengagement predicted individual differences in learning. These results provide a cohesive and statistically principled account of the dynamics of distributed and integrated circuits during cognitive processes underlying skill learning in humans.

METHODS

Methods and any associated references are available in the online version of the paper.

Note: Any Supplementary Information and Source Data files are available in the online version of the paper.

ACKNOWLEDGMENTS

D.S.B. acknowledges support from the John D. and Catherine T. MacArthur Foundation; the Alfred P. Sloan Foundation; the Army Research Laboratory (contract W911NF-10-2-0022); the Institute for Translational Medicine and Therapeutics; the US Army Research Office (contract W911NF-14-1-0679); the National Institute of Mental Health through award 2-R01-DC-009209-11; and National Science Foundation awards CRCNS BCS-1441502 and BCS-1430087 through the ENG, CISE and SBE directorates. M.Y. acknowledges support from the Applied Mathematics and Computational Science Graduate Program at the University of Pennsylvania. N.F.W. and S.T.G. were supported by PHS grant NS44393 and the Institute for Collaborative Biotechnologies through grant W911NF-09-0001 from the US Army Research Office. The content is solely the responsibility of the authors and does not necessarily represent the official views of any of the funding agencies. We thank D. Baker, S. Feldt Muldoon and Q. Telesford for comments on an earlier version of the manuscript, and we thank M.A. Porter and P.J. Mucha for helpful discussions.

AUTHOR CONTRIBUTIONS

D.S.B. formulated the project; N.F.W. and S.T.G. performed the experiments; D.S.B., N.F.W. and M.Y. did the computations; and D.S.B., M.Y., N.F.W. and S.T.G. wrote the manuscript.

COMPETING FINANCIAL INTERESTS

The authors declare no competing financial interests.

1. Ajemian, R., D'Ausilio, A., Moorman, H. & Bizzi, E. A theory for how sensorimotor skills are learned and retained in noisy and nonstationary neural circuits. *Proc. Natl. Acad. Sci. USA* **110**, E5078–E5087 (2013).
2. Grafton, S.T. & Hamilton, A.F. Evidence for a distributed hierarchy of action representation in the brain. *Hum. Mov. Sci.* **26**, 590–616 (2007).
3. Rowe, J.B. & Siebner, H.R. The motor system and its disorders. *Neuroimage* **61**, 464–477 (2012).

4. Sun, F.T., Miller, L.M., Rao, A.A. & D'Esposito, M. Functional connectivity of cortical networks involved in bimanual motor sequence learning. *Cereb. Cortex* **17**, 1227–1234 (2007).
5. Xiong, J. *et al.* Long-term motor training induced changes in regional cerebral blood flow in both task and resting states. *Neuroimage* **45**, 75–82 (2009).
6. Büchel, C., Coull, J.T. & Friston, K.J. The predictive value of changes in effective connectivity for human learning. *Science* **283**, 1538–1541 (1999).
7. Fedorenko, E. & Thompson-Schill, S.L. Reworking the language network. *Trends Cogn. Sci.* **18**, 120–126 (2014).
8. Bassett, D.S. & Bullmore, E.T. Small-world brain networks. *Neuroscientist* **12**, 512–523 (2006).
9. Bassett, D.S. & Bullmore, E.T. Human brain networks in health and disease. *Curr. Opin. Neurol.* **22**, 340–347 (2009).
10. Bassett, D.S. & Bullmore, E. *Brain Anatomy and Small-world Networks* (Betham, 2010).
11. Bullmore, E.T. & Bassett, D.S. Brain graphs: graphical models of the human brain connectome. *Annu. Rev. Clin. Psychol.* **7**, 113–140 (2011).
12. Sporns, O. *Networks of the Brain* (MIT Press, 2010).
13. Bassett, D.S. *et al.* Dynamic reconfiguration of human brain networks during learning. *Proc. Natl. Acad. Sci. USA* **108**, 7641–7646 (2011).
14. Bassett, D.S. *et al.* Task-based core-periphery structure of human brain dynamics. *PLoS Comput. Biol.* **9**, e1003171 (2013).
15. Holme, P. & Saramäki, J. Temporal networks. *Phys. Rep.* **519**, 97–125 (2012).
16. Kivelä, M. *et al.* Multilayer networks. *J. Complex Netw.* **2**, 203–271 (2014).
17. Bassett, D.S. *et al.* Robust detection of dynamic community structure in networks. *Chaos* **23**, 013142 (2013).
18. Bassett, D.S. & Lynall, M.-E. Network methods to characterize brain structure and function. In *The Cognitive Neurosciences* 5th edn (eds Gazzaniga, M.S. & Mangun, G.R.) Ch. 79 (MIT Press, 2013).
19. Doron, K.W., Bassett, D.S. & Gazzaniga, M.S. Dynamic network structure of interhemispheric coordination. *Proc. Natl. Acad. Sci. USA* **109**, 18661–18668 (2012).
20. Mantzaris, A.V. *et al.* Dynamic network centrality summarizes learning in the human brain. *J. Complex Netw.* **1**, 83–92 (2013).
21. Bassett, D.S., Wymbs, N.F., Porter, M.A., Mucha, P.J. & Grafton, S.T. Cross-linked structure of network evolution. *Chaos* **24**, 013112 (2014).
22. Logan, G.D. Toward an instance theory of automatization. *Psychol. Rev.* **95**, 492–527 (1988).
23. Hikosaka, O., Nakamura, K., Sakai, K. & Nakahara, H. Central mechanisms of motor skill learning. *Curr. Opin. Neurobiol.* **12**, 217–222 (2002).
24. Petersen, S.E., van Mier, H., Fiez, J.A. & Raichle, M.E. The effects of practice on the functional anatomy of task performance. *Proc. Natl. Acad. Sci. USA* **95**, 853–860 (1998).
25. Kelly, A.M. & Garavan, H. Human functional neuroimaging of brain changes associated with practice. *Cereb. Cortex* **15**, 1089–1102 (2005).
26. Otto, A.R., Skatova, A., Madlon-Kay, S. & Daw, N.D. Cognitive control predicts use of model-based reinforcement learning. *J. Cogn. Neurosci.* **27**, 319–333 (2015).
27. Mucha, P.J., Richardson, T., Macon, K., Porter, M.A. & Onnela, J.-P. Community structure in time-dependent, multiscale, and multiplex networks. *Science* **328**, 876–878 (2010).
28. Power, J.D. *et al.* Functional network organization of the human brain. *Neuron* **72**, 665–678 (2011).
29. Dayan, E. & Cohen, L.G. Neuroplasticity subserving motor skill learning. *Neuron* **72**, 443–454 (2011).
30. Bassett, D.S., Nelson, B.G., Mueller, B.A., Camchong, J. & Lim, K.O. Altered resting state complexity in schizophrenia. *Neuroimage* **59**, 2196–2207 (2012).
31. Floyer-Lea, A. & Matthews, P.M. Distinguishable brain activation networks for short- and long-term motor skill learning. *J. Neurophysiol.* **94**, 512–518 (2005).
32. Sakai, K. *et al.* Presupplementary motor area activation during sequence learning reflects visuo-motor association. *J. Neurosci.* **19**, RC1 (1999).
33. Grafton, S.T., Hazeltine, E. & Ivry, R.B. Motor sequence learning with the nondominant left hand. A PET functional imaging study. *Exp. Brain Res.* **146**, 369–378 (2002).
34. Honda, M. *et al.* Dynamic cortical involvement in implicit and explicit motor sequence learning. A PET study. *Brain* **121**, 2159–2173 (1998).
35. Lehéricy, S. *et al.* Distinct basal ganglia territories are engaged in early and advanced motor sequence learning. *Proc. Natl. Acad. Sci. USA* **102**, 12566–12571 (2005).
36. Siebenhühner, F., Weiss, S.A., Coppola, R., Weinberger, D.R. & Bassett, D.S. Intra- and inter-frequency brain network structure in health and schizophrenia. *PLoS ONE* **8**, e72351 (2013).
37. Patel, R., Spreng, R.N. & Turner, G.R. Functional brain changes following cognitive and motor skills training: a quantitative meta-analysis. *Neurorehabil. Neural Repair* **27**, 187–199 (2013).
38. Esslinger, C. *et al.* Neural mechanisms of a genome-wide supported psychosis variant. *Science* **324**, 605 (2009).
39. Orban, P. *et al.* The multifaceted nature of the relationship between performance and brain activity in motor sequence learning. *Neuroimage* **49**, 694–702 (2010).
40. Elton, A. & Gao, W. Divergent task-dependent functional connectivity of executive control and salience networks. *Cortex* **51**, 56–66 (2014).
41. Stoet, G. & Snyder, L.H. Neural correlates of executive control functions in the monkey. *Trends Cogn. Sci.* **13**, 228–234 (2009).
42. Shenhav, A., Botvinick, M.M. & Cohen, J.D. The expected value of control: an integrative theory of anterior cingulate cortex function. *Neuron* **79**, 217–240 (2013).
43. Chrysikou, E.G., Weber, M.J. & Thompson-Schill, S.L. A matched filter hypothesis for cognitive control. *Neuropsychologia* **62**, 341–355 (2013).
44. Thompson-Schill, S.L., Ramscar, M. & Chrysikou, E.G. Cognition without control: when a little frontal lobe goes a long way. *Curr. Dir. Psychol. Sci.* **18**, 259–263 (2009).
45. Collins, A.G. & Frank, M.J. Cognitive control over learning: creating, clustering, and generalizing task-set structure. *Psychol. Rev.* **120**, 190–229 (2013).
46. Galea, J.M., Albert, N.B., Ditye, T. & Miall, R.C. Disruption of the dorsolateral prefrontal cortex facilitates the consolidation of procedural skills. *J. Cogn. Neurosci.* **22**, 1158–1164 (2010).
47. Frey, S.H. *et al.* Neurological principles and rehabilitation of action disorders: computation, anatomy, and physiology (CAP) model. *Neurorehabil. Neural Repair* **25**, 6S–20S (2011).
48. Beeler, J.A., Petzinger, G. & Jakowec, M.W. The enemy within: propagation of aberrant corticostriatal learning to cortical function in Parkinson's disease. *Front. Neurol.* **4**, 134 (2013).
49. Cumberland Consensus Working Group *et al.* The future of restorative neurosciences in stroke: driving the translational research pipeline from basic science to rehabilitation of people after stroke. *Neurorehabil. Neural Repair* **23**, 97–107 (2009).
50. Sandrini, M. & Cohen, L.G. Noninvasive brain stimulation in neurorehabilitation. *Handb. Clin. Neurol.* **116**, 499–524 (2013).

ONLINE METHODS

Experiment and data acquisition. *Ethics statement.* Twenty-two right-handed participants (13 females and 9 males; mean age, 24 y) volunteered and provided informed consent in accordance with the guidelines of the Institutional Review Board of the University of California, Santa Barbara.

Experimental setup and procedure. We excluded two participants: one participant failed to complete the experiment, and the other had excessive head motion. Our investigation therefore included 20 participants who all had normal or corrected vision and no history of neurological disease or psychiatric disorders. This sample size is consistent with accepted good practices in this field[51]. Each participant completed a minimum of 30 behavioral training sessions, as well as three fMRI test sessions and a pretraining fMRI session. Training began immediately after the initial pretraining scan session. Test sessions occurred after every 2-week period of behavioral training, during which at least ten training sessions were required. The training was done on personal laptop computers using a training module that was installed by the experimenter (N.F.W.). Participants were given instructions on how to run the module, which they were required to do for a minimum of 10 out of the 14 d in each 2-week period. Participants were scanned on the first day of the experiment (scan 1) and approximately every 14 d after that over an approximately 42-d period (scans 2–4).

We asked participants to practice a set of ten-element sequences in a discrete sequence-production (DSP) task in which the participants generated responses to sequential, visually presented stimuli (**Supplementary Fig. 1**) by using a laptop keyboard with their right hand. Sequences were presented using a horizontal array of five square stimuli; the responses were mapped from left to right, such that the thumb corresponded to the leftmost stimulus and the smallest finger corresponded to the rightmost stimulus. A square highlighted in red served as the imperative stimulus, and the next square in the sequence was highlighted immediately after each correct key press. If an incorrect key was pressed, the sequence was paused at the error and restarted upon the appropriate key press.

Participants had an unlimited amount of time to respond and to complete each trial. All participants trained on the same set of six different ten-element sequences, which were presented with three different levels of exposure. Each stimulus location was presented twice and included neither stimulus repetition (for example, "11" could not occur) nor regularities such as trills (for example, "121") or runs (for example, "123"). Each training session (**Supplementary Fig. 2**) included two extensively trained (EXT) sequences that were each practiced for 64 trials, two moderately trained (MOD) sequences that were each practiced for 10 trials, and two minimally trained (MIN) sequences that were each practiced for 1 trial. (See **Table 2** for the number of trials of each sequence type.) Each trial began with the presentation of a sequence-identity cue. The purpose of the identity cue was to tell the participant what sequence would have to be typed. For example, the EXT sequences were preceded by either a cyan (sequence A) or a magenta (sequence B) circle. Participants also saw identity cues for the MOD sequences (red or green triangles) and the MIN sequences (orange or white stars, each of which was outlined in black). No participant reported any difficulty viewing the different identity cues. Feedback regarding the number of error-free sequences that the participant produced and the mean time required to complete an error-free sequence was presented after every block of ten trials.

Each fMRI test session was completed after approximately ten home training sessions, and each participant took part in three test sessions. Each participant had a pretraining scan session that was identical to the other test scan sessions immediately before the start of training (**Supplementary Fig. 2**). To familiarize participants with the task, we gave a brief introduction before the start of the pretraining session. We showed the participants the mapping between the fingers and the DSP stimuli, and we explained the significance of the sequence-identity cues.

To help ease the transition between each participant's training environment and that of the scanner, we placed padding under the participant's knees to maximize comfort. Participants made responses using a fiber optic response box that was designed with a configuration of buttons similar to those found on the typical laptop used during training (**Supplementary Fig. 1**). For instance, the center-to-center spacing between the buttons on the top row was 20 mm (compared to 20 mm from "G" to "H" on a recent version of the MacBook Pro), and the spacing between the top row and lower left 'thumb' button was 32 mm (compared to 37 mm from "G" to the spacebar on a MacBook Pro). The response box was supported with a board whose position could be adjusted to accommodate a participant's reach and hand size. Additional padding was placed under the right forearm to minimize muscle strain during the task. To minimize head motion, we inserted padded wedges between the participant and the head coil of the MRI scanner. The number of sequence trials performed during each scanning session was the same for all participants, except for two abbreviated sessions that resulted from technical problems. In each case when scanning was cut short, participants completed four out of the five scan runs for a given session. We included data from these abbreviated sessions in this study.

Participants were tested inside of the scanner with the same DSP task and the same six sequences they had practiced during training. Participants were given unlimited time to complete trials and were instructed to respond quickly and maintain accuracy. Trial completion was signified by the visual presentation of a fixation mark, "+," which remained on the screen until the onset of the next sequence-identity cue. To ensure a sufficient number of events for each exposure type, all sequences were presented with the same frequency. As in the training, trials were organized into blocks of ten and were followed by performance feedback. Each block contained trials belonging to a single exposure type and included five trials for each sequence. Trials were separated by an intertrial interval that lasted between 0 and 6 s (not including any time remaining from the previous trial). Scan epochs contained 60 trials (i.e., six blocks) and consisted of 20 trials for each exposure type. Each test session contained five scan epochs, yielding a total of 300 trials and a variable number of brain scans depending on how quickly the task was performed.

Behavioral apparatus. Stimulus presentation was controlled during training using participants' laptop computers, which were running Octave 3.2.4 in conjunction with Psychtoolbox version 3. We controlled test sessions using a laptop computer running MATLAB version 7.1 (Mathworks, Natick, MA). We collected key-press responses and response times using a custom fiber optic button box and transducer connected via a serial port (button box, HHSC-1 × 4-l; transducer, fORP932; Current Designs, Philadelphia, PA).

Behavioral estimates of learning. To ensure independence of brain network organization and learning, we extracted brain network structures during the four scanning sessions, and we extracted behavioral estimates of learning in home training sessions across the 6 weeks of practice.

For each sequence, we defined the movement time (MT) as the difference between the time of the first button press and the time of the last button press in a single sequence. For the set of sequences of a single type (i.e., sequence 1, 2, 3, 4, 5 or 6), we estimated the learning rate by fitting a double exponential function to the MT data[52,53] using a robust outlier correction in MATLAB (using the function "fit.m" in the Curve Fitting Toolbox with option "Robust" and type "Lar"): $MT = D_1 e^{-t\kappa} + D_2 e^{-t\lambda}$, where t is time, κ is the exponential drop-off parameter (which we called the learning rate) used to describe the fast rate of improvement, λ is the exponential drop-off parameter used to describe the slow, sustained rate of improvement, and D_1 and D_2 are real and positive constants. The magnitude of κ indicates the steepness of the learning slope: individuals with larger κ values have a steeper drop-off in MT, suggesting that they are quicker learners[29,54]. The decrease in MT has been used to quantify learning for several decades[55,56]. Several functional forms have been suggested for the fit of MT[57,58], and variants of an exponential are viewed as the most statistically robust choices[58]. In addition, the fitting approach that we used has the advantage of estimating the rate of learning independently of initial performance or performance ceiling.

fMRI imaging. *Imaging procedures.* We acquired signals using a 3.0 T Siemens Trio with a 12-channel phased-array head coil. For each whole-brain scan epoch, we used a single-shot echo planar imaging sequence that was sensitive to BOLD contrast to acquire 37 slices per repetition time (repetition time (TR) of 2,000 ms, 3-mm thickness, 0.5-mm gap) with an echo time of 30 ms, a flip angle of 90°, a field of view of 192 mm, and a 64 × 64 acquisition matrix. Before the collection of the first functional epoch, we acquired a high-resolution T1-weighted sagittal sequence image of the whole brain (TR of 15.0 ms, echo time of 4.2 ms, flip angle of 9°, 3D acquisition, field of view of 256 mm, slice thickness of 0.89 mm, and 256 × 256 acquisition matrix).

fMRI data preprocessing. We processed and analyzed functional imaging data using Statistical Parametric Mapping (SPM8, Wellcome Trust Center for Neuroimaging and University College London, UK). We first realigned raw functional data, then coregistered it to the native T1 (normalized to the MNI-152 template with a resliced resolution of 3 × 3 × 3 mm), and finally smoothed it using

doi:10.1038/nn.3993

an isotropic Gaussian kernel of 8-mm full width at half-maximum. To control for fluctuations in signal intensity, we normalized the global intensity across all functional volumes. Using this pipeline of standard realignment, coregistration, normalization and smoothing, we were able to correct for motion effects due to volume-volume fluctuations relative to the first volume in a scan run. The global signal was not regressed out of voxel time series, given its controversial application to resting-state fMRI data[59–61] and the lack of evidence of its utility in analyses of task-based fMRI data. Moreover, the functional connectivity matrices that we produced (see the section "Network construction") did not show evidence of strong global functional correlations, but instead showed discrete organization in motor, visual and non-motor, non-visual areas.

After this motion-correction procedure, we observed no correlation between any of the six motion parameters (*x*-translation, *y*-translation, *z*-translation, roll, pitch and yaw, calculated for each run and training session) and either motor-visual integration or non-motor, non-visual recruitment ($P > 0.05$, corrected for multiple comparisons using a false-discovery-rate correction) across all scanning sessions. These results indicated that individual differences in motion were unlikely to drive individual differences in observed network structures after motion correction.

General linear model. Supplementary Figure 9 compares results obtained from functional connectivity to insights provided by a general linear model (GLM). We performed a standard GLM analysis to quantify the degree to which brain regions showed a linear decrease in activity over the course of training, and then we asked whether average beta-weights of this GLM were different between functional modules. For each subject, the BOLD response was modeled using a single design matrix with parameters estimated using the GLM. We used an event-related design to model the expression of sequence-specific representations, with trial onset corresponding to the presentation of the sequence identity cue, 2 s before the presentation of the initial DSP target stimulus. This approach included both the preparation and the production of learned sequences. We constructed the design matrix for each subject using separate factors for each scan session (pre-training session and training sessions 1–3), exposure condition (MIN, MOD and EXT) and repetition (new or repeated trial). For a trial to be coded as a repeated event, the previous trial had to have been (i) of the exact same sequence and (ii) performed correctly. Repeated trials that followed error trials, as well as the error trials themselves, were modeled using a separate column in the design matrix. To account for nonspecific effects of sessions, blocking variables were included for each scan run. Potential differences in BOLD values due to MT-related kinematics were accounted for by using the MT from each trial as the trial duration for modeled events[62]. To control for the potential influence of the time between trials, we weighted each event by the time elapsed since the previous trial. Following center mean normalization, this column was added to the model as a covariate of non-interest. Events were convolved using the canonical hemodynamic response function and temporal derivative in SPM8. Using freely available software[63], we then combined corresponding beta image pairs for each event type (hemodynamic response function and temporal derivative) at the voxel level to form a magnitude image[64]. To generate linear contrast images at the individual-subject level, we multiplied magnitude images corresponding to conditions of interest by the appropriate contrast weight and then combined them through addition. We then averaged the beta weights of all voxels within a given region.

Network construction. *Partitioning the brain into regions of interest.* In studies of the functional connectivity between brain areas, it is common to apply a standardized atlas to raw fMRI data[8,9,65]. The choice of atlas or parcellation scheme is the topic of several recent studies on structural[66,67], resting-state[68] and task-based[28] network architecture, and it is guided by the particular scientific question at hand[11,69].

Consistent with previous studies of task-based functional connectivity during learning[13,14,17,20,21], we parcellated the brain into 112 cortical and subcortical regions using the structural Harvard-Oxford (HO) atlas of the FMRIB (Oxford Centre for Functional Magnetic Resonance Imaging of the Brain) Software Library[70,71] (FSL; Version 4.1.1). **Supplementary Figures 10–13** show that our results were robust in a finer grained template created by the combination of two separate atlases: (i) the automated anatomical labeling (AAL)-derived 600-region atlas that we developed for use previously[72,73], which subdivides the 90 AAL regions into regions of roughly similar size via a spatial-bisection method, and (ii) a high-resolution probabilistic 26-region atlas of the cerebellum in the anatomical space defined by the MNI152 template, obtained from T1-weighted MRI scans (1-mm isotropic resolution) of 20 healthy, young participants[74,75]. For each individual participant and each of the 112 regions, we determined the regional mean BOLD time series by separately averaging across all of the voxels in that region.

Within each HO-atlas region, we constrained voxel selection to voxels that were located within an individual participant's gray matter. To do this, we first segmented each individual participant's T1 into white- and gray-matter volumes using the DARTEL toolbox in SPM8. We then restricted the gray-matter voxels to those with an intensity of 0.3 or more (the maximum intensity was 1.0 (arbitrary units)). We then spatially normalized the participant T1 and corresponding gray-matter volume to the MNI152 template using the standard SPM 12-parameter affine registration and resampled to 3-mm isotropic voxels. We then restricted the voxels for each HO region using the program fslmaths[70,71] to include only voxels that were in the individual participant's gray-matter template.

Wavelet decomposition. Wavelet decompositions of fMRI time series have been applied extensively to fMRI data[76,77], where they sensitively detect small signal changes in nonstationary time series with noisy backgrounds[78]. We used the maximum-overlap discrete wavelet transform, which has been used extensively in functional connectivity studies[79–84], to decompose regional time series into wavelet scales corresponding to specific frequency bands[85].

We were interested in quantifying correlations between task-based fMRI signals indicative of cooperative temporal dynamics. Because our sampling frequency was 2 s (1 TR), wavelet scale 1 corresponded to 0.125–0.25 Hz, and scale 2 to 0.06–0.125 Hz. Previous work demonstrates that functional associations between low-frequency components of the fMRI signal (0–0.15 Hz) can be attributed to task-related functional connectivity, whereas associations between high-frequency components (0.2–0.4 Hz) cannot[86]. This frequency specificity is probably due in part to the hemodynamic response function, which might act as a noninvertible band-pass filter for underlying neural activity[86]. Consistent with our previous work[13,14,21], we examined wavelet scale 2, which is thought to be particularly sensitive to dynamic changes in task-related functional brain architecture.

Construction of dynamic networks. For each of the 112 brain regions, we extracted the wavelet coefficients of the mean time series in temporal windows given by trial blocks (of approximately 60 TRs). We thereby extracted block-specific data sets from the EXT, MOD and MIN sequences (with six to ten blocks of each sequence type) for each of the 20 participants and four scanning sessions. For each block-specific data set, we constructed an $N \times N$ adjacency matrix $\boldsymbol{W}$ representing the set of pairwise functional connections in that window for a given participant and a given scan. To quantify the weight W_{ij} of the functional connectivity between regions i and j, we used the magnitude-squared spectral coherence (consistent with our previous study[13]). By using the coherence, which has been shown to be useful in the context of fMRI neuroimaging data[86], we were able to measure frequency-specific linear relationships between time series.

To examine changes in functional brain-network architecture during learning, we constructed multilayer networks by considering the set of L adjacency matrices constructed from consecutive blocks of a given sequence type (EXT, MOD or MIN) for a given participant and scanning session. We combined the matrices in each set separately to form a rank-3 adjacency tensor $\boldsymbol{A}$ per sequence type, participant and scan. Such a tensor can be used to represent a time-dependent network[13,14,27]. The **Supplementary Note** contains details on the dynamic network clustering method used to extract putative functional modules as participants performed the task.

A **Supplementary Methods Checklist** is available.

51. Desmond, J.E. & Glover, G.H. Estimating sample size in functional MRI (fMRI) neuroimaging studies: statistical power analyses. *J. Neurosci. Methods* **118**, 115–128 (2002).
52. Schmidt, R.A. & Lee, T.D. *Motor Control and Learning: A Behavioral Emphasis* 4th edn (Human Kinetics, 2005).
53. Rosenbaum, D.A. *Human Motor Control* (Elsevier, 2010).
54. Yarrow, K., Brown, P. & Krakauer, J.W. Inside the brain of an elite athlete: the neural processes that support high achievement in sports. *Nat. Rev. Neurosci.* **10**, 585–596 (2009).
55. Snoddy, G.S. Learning and stability: a psychophysical analysis of a case of motor learning with clinical applications. *J. Appl. Psychol.* **10**, 1–36 (1926).

56. Crossman, E.R.F.W. A theory of the acquisition of speed-skill. *Ergonomics* **2**, 153–166 (1959).
57. Newell, K.M. & Rosenbloom, P.S. Mechanisms of skill acquisition and the law of practice. In *Cognitive Skills and Their Acquisition* (ed Anderson, J.R.) 1–55 (Lawrence Erlbaum Associates, 1981).
58. Heathcote, A., Brown, S. & Mewhort, D.J. The power law repealed: the case for an exponential law of practice. *Psychon. Bull. Rev.* **7**, 185–207 (2000).
59. Murphy, K., Birn, R.M., Handwerker, D.A., Jones, T.B. & Bandettini, P.A. The impact of global signal regression on resting state correlations: are anti-correlated networks introduced? *Neuroimage* **44**, 893–905 (2009).
60. Saad, Z.S. *et al.* Trouble at rest: how correlation patterns and group differences become distorted after global signal regression. *Brain Connect.* **2**, 25–32 (2012).
61. Chai, X.J., Castañón, A.N., Ongür, D. & Whitfield-Gabrieli, S. Anticorrelations in resting state networks without global signal regression. *Neuroimage* **59**, 1420–1428 (2012).
62. Grinband, J., Wager, T.D., Lindquist, M., Ferrera, V.P. & Hirsch, J. Detection of time-varying signals in event-related fMRI designs. *Neuroimage* **43**, 509–520 (2008).
63. Steffener, J., Tabert, M., Reuben, A. & Stern, Y. Investigating hemodynamic response variability at the group level using basis functions. *Neuroimage* **49**, 2113–2122 (2010).
64. Calhoun, V.D., Stevens, M.C., Pearlson, G.D. & Kiehl, K.A. fMRI analysis with the general linear model: removal of latency-induced amplitude bias by incorporation of hemodynamic derivative terms. *Neuroimage* **22**, 252–257 (2004).
65. Bullmore, E. & Sporns, O. Complex brain networks: graph theoretical analysis of structural and functional systems. *Nat. Rev. Neurosci.* **10**, 186–198 (2009).
66. Bassett, D.S., Brown, J.A., Deshpande, V., Carlson, J.M. & Grafton, S.T. Conserved and variable architecture of human white matter connectivity. *Neuroimage* **54**, 1262–1279 (2011).
67. Zalesky, A. *et al.* Whole-brain anatomical networks: does the choice of nodes matter? *Neuroimage* **50**, 970–983 (2010).
68. Wang, J. *et al.* Parcellation-dependent small-world brain functional networks: a resting-state fMRI study. *Hum. Brain Mapp.* **30**, 1511–1523 (2009).
69. Wig, G.S., Schlaggar, B.L. & Petersen, S.E. Concepts and principles in the analysis of brain networks. *Ann. NY Acad. Sci.* **1224**, 126–146 (2011).
70. Smith, S.M. *et al.* Advances in functional and structural MR image analysis and implementation as FSL. *Neuroimage* **23**, S208–S219 (2004).
71. Woolrich, M.W. *et al.* Bayesian analysis of neuroimaging data in FSL. *Neuroimage* **45**, S173–S186 (2009).
72. Hermundstad, A.M. *et al.* Structural foundations of resting-state and task-based neural activity in the human brain. *Proc. Natl. Acad. Sci. USA* **110**, 6169–6174 (2013).
73. Hermundstad, A.M. *et al.* Structurally-constrained relationships between cognitive states in the human brain. *PLoS Comput. Biol.* **10**, e1003591 (2014).
74. Diedrichsen, J., Balster, J.H., Flavell, J., Cussans, E. & Ramnani, N. A probabilistic MR atlas of the human cerebellum. *Neuroimage* **46**, 39–46 (2009).
75. Diedrichsen, J. *et al.* Imaging the deep cerebellar nuclei: a probabilistic atlas and normalization procedure. *Neuroimage* **54**, 1786–1794 (2011).
76. Bullmore, E. *et al.* Wavelets and statistical analysis of functional magnetic resonance images of the human brain. *Stat. Methods Med. Res.* **12**, 375–399 (2003).
77. Bullmore, E. *et al.* Wavelets and functional magnetic resonance imaging of the human brain. *Neuroimage* **23**, S234–S249 (2004).
78. Brammer, M.J. Multidimensional wavelet analysis of functional magnetic resonance images. *Hum. Brain Mapp.* **6**, 378–382 (1998).
79. Achard, S., Salvador, R., Whitcher, B., Suckling, J. & Bullmore, E. A resilient, low-frequency, small-world human brain functional network with highly connected association cortical hubs. *J. Neurosci.* **26**, 63–72 (2006).
80. Bassett, D.S., Meyer-Lindenberg, A., Achard, S., Duke, T. & Bullmore, E. Adaptive reconfiguration of fractal small-world human brain functional networks. *Proc. Natl. Acad. Sci. USA* **103**, 19518–19523 (2006).
81. Achard, S. & Bullmore, E. Efficiency and cost of economical brain functional networks. *PLoS Comput. Biol.* **3**, e17 (2007).
82. Achard, S., Bassett, D.S., Meyer-Lindenberg, A. & Bullmore, E. Fractal connectivity of long-memory networks. *Phys. Rev. E* **77**, 036104 (2008).
83. Bassett, D.S., Meyer-Lindenberg, A., Weinberger, D.R., Coppola, R. & Bullmore, E. Cognitive fitness of cost-efficient brain functional networks. *Proc. Natl. Acad. Sci. USA* **106**, 11747–11752 (2009).
84. Lynall, M.E. *et al.* Functional connectivity and brain networks in schizophrenia. *J. Neurosci.* **30**, 9477–9487 (2010).
85. Percival, D.B. & Walden, A.T. *Wavelet Methods for Time Series Analysis* (Cambridge University Press, 2000).
86. Sun, F.T., Miller, L.M. & D'Esposito, M. Measuring interregional functional connectivity using coherence and partial coherence analyses of fMRI data. *Neuroimage* **21**, 647–658 (2004).

doi:10.1038/nn.3993